Modeling Variation in Multi-station Compliant Assembly using Parametric Space Envelope

Chen Luo[1]
Department of Mechanical Engineering
Southeast University
Nanjing, China; 211189
chenluo@seu.edu.cn

Jiaqi Nie
Department of Mechanical Engineering
Southeast University
Nanjing, China; 211189
jiaqinie@seu.edu.cn

Pasquale Franciosa
WMG, the International Manufacturing Centre
University of Warwick
Coventry/UK; CV4 7AL
P.Franciosa@warwick.ac.uk

Dariusz Ceglarek
WMG, the International Manufacturing Centre
University of Warwick
Coventry/UK; CV4 7AL
D.J.Ceglarek@warwick.ac.uk

[1] Corresponding author

Abstract

Non-rigid compliant parts are widely used in industries. One of the biggest challenges facing industries is geometric variation management of these compliant parts which can directly impact product quality and functionality. Existing rigid body-based variation modeling approaches are not suitable for compliant assembly while finite element analysis based methods have the disadvantage of requiring heavy computation efforts and detailed design information which is unavailable during preliminary design phase. Hence, this paper develops a novel methodology to evaluate geometric variation propagation in multi-station compliant assembly based on parametric space envelope (i.e. variation tool constructed from parametric curves). Three sources of variation: location-led positional variation, assembly deformation-induced variation and station transition caused variation are analyzed. In this study, geometric variations are modeled indirectly through a compact set of boundary control points. Compared with existing methods where geometric variation is modeled by tracking key feature points on the manufacturing part, the proposed approach brings many benefits. It can handle arbitrary complex compliant part, and it lowers computation requirement in many real applications. The method is illustrated and verified through an industrial case study on a multi-station compliant panel assembly. The developed method provides industries a new way to manage geometric variation from compliant assembly.

***Keywords**: Compliant assembly, geometric variation, variation propagation, geometric variation modeling*

1. Introduction

Compliant parts are widely used in many industries including aerospace, automotive, appliance and electronics, and ship-building [1, 2]. Compliant assembly is a manufacturing process where two or more non-rigid parts are joined together using various joining techniques following place-clamp-fasten-release (PCFR) cycle within a single or multiple assembly station [3]. The result of this process is a subassembly or a final product. One of the most prominent challenges facing compliant assembly engineers entails geometric variation management. An excessive geometric variation of these non-rigid parts can lead to numerous quality related problems such as (i) high rate of re-work or scrap, (ii) inferior product functional performance, (iii) tooling failures, and (iv) unexpected production downtime which, in turn, reduces both product quality and production throughput [1].

Geometric variation can stem from manufacturing as well as the design of a product. Manufacturing induced variation is inevitable. Therefore, it is vital to minimize both design-inherent as well as process-induced level of geometric variation. To achieve this, a thorough assessment of the manufacturing process is required when designing the product and make decision on choosing assembly operations. However, assessing multistage systems present significant challenges for the manufacturing industry [4]. In most cases, the quality of the final product generated out of a multistage system is determined by complex interactions among multiple stages—the quality characteristics at one stage are not only impacted by local variations at that stage, but also by variations propagated from upstream stages.

Clearly, understanding how assembly variation propagates in a multi-station assembly system is of critical importance to improve the final product quality. In addition, a better understanding of a process behavior can lead to reduction in the time needed to launch a new product. Further, accurate evaluations of inherent process variation in preliminary assembly phase are key to reducing manufacturing costs [5].

Due to the variability of the parts [6], fixtures [7-11] and joining methods [12, 13] in each station and their interactions, multi-station assembly process can be considered as a complex variation ‘‘stack up’’ process. Dimensional variation modeling and analysis for multi-station manufacturing processes have been conducted mainly for rigid parts: 2D [14] and 3D [15]. Comparatively limited research has been done on multi-station systems

considering compliant, non-rigid parts. Some researchers have attempted to modify the existing rigid-body propagation model by adding elastic deformation variation component [16]. However, the treatment is incomplete and the effectiveness and accuracy of the modified methods are case dependent. To tackle non-rigid part deformation, finite element method (FEM) has been introduced by researchers [17, 18] into multi-stage manufacturing system as a valid tool to model assembly variation. However, FEM based approaches require huge computation efforts in many real applications.

In general, the aforementioned variation propagation methods model and track characteristic points' move along the assembly chain to the final product. However, to completely describe the real part shape it will be necessary to know a very large infinite number of points (point cloud). As such only a limited number of points are selected in real application. Such key characteristic points typically include welding position points, fixture points and other locating points [19, 20]. This presents significant problem, in terms of processing time and modeling accuracy, when applying these methods to compliant part with complex shapes. In the light of aforesaid discussion, this paper proposes a novel methodology for modeling geometric variation for multi-station compliant assembly based on the concept of *parametric space envelope* (PSE). In this study, geometric variations' accumulation and propagation through multi-station assembly process is mathematically modeled through envelope's boundary control points' displacements. This indirect approach brings modeling accuracy and computation efficiency. For example, the user is able to add dozen extra control points to improve modeling accuracy compared with adding thousands more characteristic points under existing methods. The developed method incorporates nonlinear compliant part's deformation modeling as well as variation propagation modeling from different subassemblies to the final product. It provides industries a new way to manage geometric variation on compliant assembly.

The remainder of this paper is organized as follows. Section 2 provides related work on assembly variation modeling. Sections 3 and 4 present the proposed methodology on compliant assembly variation modeling based upon parametric space envelope. An industrial case study is provided in Section 5 on a two-stage three parts assembly using proposed methodology. Discussions on developed methodology are provided in Section 6. Section 7

concludes the analysis and points the direction for future research.

2. Related Work

Geometric variation management plays an important role in product quality and functionality. This area has seen considerable amount of research interests. Dimensional variation modeling and analysis for rigid parts in multi-station manufacturing processes have been extensively studied. Jin and Shi [14] and Ding et al. [21] proposed a state space modeling approach for dimensional control of sheet metal assembly process with 2D parts extended to 3D parts by Huang et al. [15], where the state equation considers two types of dimensional variation, the part error itself and the fixture error. Mantripragada and Whitney [22] proposed a variation propagation model using state transition models. Both [22] and [15] approaches consider rigid parts and the state space vector can be fully described by translation and re-orientation. The state transition model allows the application of control systems theory to analyze multi-station assembly system.

Different from the above methods, Lawless et al. [23] put forth a time series-based method called Variation Driver Analysis. The method tracks the characteristics of individual parts as they pass through multiple stations using autoregressive models. More recently, Li et al. [24] applied the state space model to the remanufacturing assembly where the quality control issue is transformed into a convex quadratic programming. Yacob and Semere [25] proposed an artificial intelligence based approach to predict geometrical deviations of parts given manufacturing errors. The neural network model is trained on simulated data, generated from machining simulation of a point cloud of a part.

As more non-rigid parts enter into production, deformation of these compliant parts plays an important role in geometric variation. Rigid part models do not consider part deformation during assembly so that the part and tooling variation can be solely represented by kinematic relationships. As such, rigid body models cannot be applied to the compliant metal plate assemblies leading researcher to develop new methods targeting compliant assembly where the deformation of the parts during the assembly process is considered. Liu and Hu [26] and Shahi et al. [27] developed a model to evaluate the spot weld sequence in sheet metal assembly. This model considers a process where welding is carried out in multiple

stages. In contrast, Chang and Gossard [28] presented a graphic approach for multi-station assembly of compliant parts.

Focusing on single station, Liu and Hu [17] and Liu et al. [29] proposed the method of influence coefficients (MIC) to analyze the impact of deformation and springback on assembly variation by applying linear mechanics and statistics. Using finite element methods, they built a sensitivity matrix for compliant parts of complex shapes. The sensitivity matrix establishes the linear relationship between the incoming part deviation and output assembly deviation. Based on MIC, Li et al. [30] developed a multilevel optimization methodology for product (parts and subassemblies) and process tolerance allocation in multi-station compliant assembly. They modeled multi-station compliant assembly as a hierarchical multilevel process. Then they used analytical target cascading to formulate and solve the multilevel tolerance allocation optimization problem. This decomposition-based approach translates final product quality and cost targets to tolerance specifications for incoming parts, subassemblies, and station fixtures. Huang and Ceglarek [31] and Huang et al. [32] presented a discrete cosine-transformation (DCT) based decomposition method for modeling and control of compliant assemblies form error. The method decomposes the dimensional error field into a series of independent error modes.

To tackle multi-station compliant assembly, Camelio et al. applied component geometric covariance to the multi-stage assembly variation propagation analysis [20, 33]. They considered different variation sources including part variation, fixture variation, and welding gun variation. The stream of variation (SOVA) theory in variation propagation modeling for multistage machining and assembly processes is popular with practitioner [15, 34]. Zhang and Shi developed a variation propagation model for stream of variation analysis in a multi-station assembly process for composite parts [35]. The method considers major variation factors, including part manufacturing error, fixture position error, and relocation-induced error. Taking benefits of finite element method, a state space model is established to represent the relationships between the sources of variation and the final assembly variation. The SOVA method is originally designed to tackle rigid body workpiece variation management. Recently, Wang et al. [16] incorporated elastic deformation variations to the SOVA method and applied it to analyze variable stiffness structure workpieces. Addressing dimensional quality, Jandaghi

and Masoumi proposed a variation propagation model on sheet metal parts in multi-station assembly system [36]. In this method, three sources of deviations—non-ideal parts, fixture errors, and assembly operations effects—are taken into account. It adopted SOVA to model rigid variation while applying variation response methodology (VRM) to analyze compliant variation with non-ideal parts [37, 38]. However, similar to other methods, this method has the general limitation and application hurdle surrounding simulation costs and complexities and requires detailed information about part geometry and assembly process.

From reviewing existing methods, steady progress has been made on manufacturing parts' geometric variation modeling. However, there are still demands from industries for new methods to tackle multi-station systems considering compliant, non-rigid parts especially in early/preliminary design phases. To address the gap, this paper proposes a novel variation model for multi-station compliant assembly based on purpose built variation tool termed *parametric space envelope (PSE)*.

3. Assembly Variation

Parametric space envelope (PSE) [39] is a useful shape editing technique for geometric modeling. Under this technique, a *parametric space envelope* is constructed using base parametric curves (i.e. Bezier curves used in this paper, but also B-splines, nonuniform rational basis spline (NURBS)). The embedded manufacturing part $\boldsymbol{Q}_{\mathrm{B}}(u,v,w)$ is linked to a compact set of control points $\boldsymbol{p}_{ijk}$ through:

$$\boldsymbol{Q}_{\mathrm{B}}(u,v,w)=\sum_{i=0}^{l}\sum_{j=0}^{m}\sum_{k=0}^{n}B_i^l(u)B_j^m(v)B_k^n(w)\cdot\boldsymbol{p}_{ijk} \tag{1}$$

where $B_i^l(u), B_j^m(v),$ and $B_k^n(w)$ are Bernstein basis functions. Under the design, embedded object's deviation and deformation can be modeled through control points' movement. Leveraging this technique, the methodology developed in this paper can not only model rigid part's transitional and rotational deviations but also non-rigid part deformations occurred during assembly. In general, there is inevitable manufacturing part variation during the assembly. The main sources of the variations include fixture error, the transfer of assembly parts between the stations, as well as random errors introduced during the assembly process.

3.1 Fixture Error. In compliant assembly, fixture error causes assembly deviation. This is driven mainly by two factors. One is that locators of fixture deviate from nominal position causing assembly deviation [5, 6, 8]. The other is that fixture can also deform the flexible parts, such as part spring back after releasing the clamps. Under proposed method, these two types of deviation are modeled. Under coordinate system, control point perturbation at station k is represented by U. $U1$ represents control point displacement caused by manufacturing part positional deviation, and $U2$ represents control point displacement caused by part's deformation in an assembly involving r parts:

$$\boldsymbol{U}1_i(k)=\begin{bmatrix} u1_{111ix} & \cdots & u1_{lmnix} & \cdots & u1_{Npix} \\ u1_{111iy} & \cdots & u1_{lmniy} & \cdots & u1_{Npiy} \\ u1_{111iz} & \cdots & u1_{lmniz} & \cdots & u1_{Npiz} \\ 0 & \cdots & 0 & \cdots & 0 \end{bmatrix}_{4\times Npi} \quad i=1,\cdots,r \tag{2}$$

$$\boldsymbol{U}2_i(k)=\begin{bmatrix} u2_{111ix} & \cdots & u2_{lmnix} & \cdots & u2_{Npix} \\ u2_{111iy} & \cdots & u2_{lmniy} & \cdots & u2_{Npiy} \\ u2_{111iz} & \cdots & u2_{lmniz} & \cdots & u2_{Npiz} \\ 0 & \cdots & 0 & \cdots & 0 \end{bmatrix}_{4\times Npi} \quad i=1,\cdots,r \tag{3}$$

where $u1_{lmnix}$, $u1_{lmniy}$, and $u1_{lmniz}$ represent the displacement of the *(l-m-n)*th control point along x, y and z-axis from part positional deviation; Similarly $u2_{lmnix}$, $u2_{lmniy}$, $u2_{lmniz}$ represent the (*l-m-n)*th control point displacement caused by the part deformation. The index N_{pi} =(l+1)×(m+1)×(n+1) represents the total number of control points. This is illustrated in Fig. 1 where sheet metal's dislocation and deformation are modeled through *PSE* boundary control points' displacement. Fig. 1(a) shows sheet metal part is placed into a variation tool, i.e., a Bezier volume of degree l=2, m=2, and n=1 defined by a set of (l + 1)×(m + 1)×(n + 1) =18 control points P_{ijk} with 3 in x-direction, 3 in y-direction and 2 in z-direction. Since $\boldsymbol{U}1$ and $\boldsymbol{U}2$ are both control point perturbation in the same coordinate system, they are additive:

$$\boldsymbol{U}=\boldsymbol{U}1+\boldsymbol{U}2 \tag{4}$$

$$\boldsymbol{U}_i(k)=\begin{bmatrix} u_{111ix} & \cdots & u_{lmniz} & \cdots & u_{Npix} \\ u_{111iy} & \cdots & u_{lmniz} & \cdots & u_{Npiy} \\ u_{111iz} & \cdots & u_{lmniz} & \cdots & u_{Npiz} \\ 0 & \cdots & 0 & \cdots & 0 \end{bmatrix}_{4\times Npi} \tag{5}$$

where u_{lmnix}, u_{lmniy}, and u_{lmniz} $(i=1,\cdots,r)$ represent the displacement of the *l*-*m*-*n*th control point in the *x*, *y*, and *z*-directions, respectively.

The control point displacement of *r* assembly parts in the coordinate system at station *k* can be expressed as:

$$\boldsymbol{U}(k)=\begin{bmatrix} \boldsymbol{U}_1(k) & & & \\ & \boldsymbol{U}_2(k) & & \\ & & \ddots & \\ & & & \boldsymbol{U}_r(k) \end{bmatrix}_{4r\times(Np1+\cdots+Npr)} \tag{6}$$

If there are already r_k parts at station *k*, the assembled substructure is affected by the fixture error similar to one object, i.e., $\boldsymbol{U}_1(k)=\boldsymbol{U}_2(k)=\cdots=\boldsymbol{U}_{r_{k-1}}(k)$. Those parts not involved at station *k* are represented with zero matrix, i.e., $\boldsymbol{U}_{r_{k+1}}(k)$, $\boldsymbol{U}_{r_{k+2}}(k)$, ⋯, $\boldsymbol{U}_r(k)$ are $\boldsymbol{O}_{4\times Npr_{k+1}},\boldsymbol{O}_{4\times Npr_{k+2}},\cdots,\boldsymbol{O}_{4\times Npr}$ respectively.

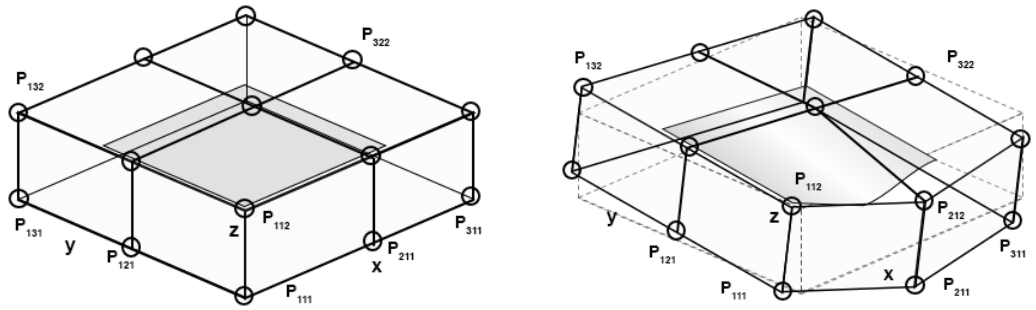

(*a*) (*b*)

Fig. 1 Fixture error caused compliant part deviation and deformation are modeled through control points' displacement: (*a*) ideal state with no control point displacement when sheet metal stays at nominal position, (*b*) fixture errors cause sheet metal deviation and stretch deformation, and these two types of variation can be modeled through control points' displacement.

3.2 Reorientation Error. In multi-station assembly, reorientation error introduced by Shiu et al. [40] refers to part/subassembly variation caused by changing tooling layout from station $k-1$ to station *k* for locating the datum part (i.e., the part which is positioned by the datums to the design nominal on each station; in general, this is the first part located in a

given station). The parts are positioned according to consecutive station's locating scheme. Therefore, the subassembly is "re-oriented" according to the next station's tooling layout. The reorientation matrix is applied as transformation matrix to describe the position transfer when the part is reoriented. Rigid body transformation of the embedded parts can be represented by the transformation of the control points. As shown in Fig. 2, the reorientation is realized by the translation and rotation of the control points. The reorientation matrix can be expressed as:

$$\boldsymbol{A}_i(k) = \boldsymbol{T}_{\boldsymbol{A}i}^{-1}(k) \cdot \boldsymbol{R}_{\boldsymbol{A}i}(k) \cdot \boldsymbol{T}_{\boldsymbol{A}i}(k) \tag{7}$$

where $\boldsymbol{T}_{\boldsymbol{A}i}(k) = \begin{bmatrix} 1 & 0 & 0 & -x_{ik} \\ 0 & 1 & 0 & -y_{ik} \\ 0 & 0 & 1 & -z_{ik} \\ 0 & 0 & 0 & 1 \end{bmatrix}$, $\boldsymbol{T}_{\boldsymbol{A}i}^{-1}(k) = \begin{bmatrix} 1 & 0 & 0 & x_{ik} \\ 0 & 1 & 0 & y_{ik} \\ 0 & 0 & 1 & z_{ik} \\ 0 & 0 & 0 & 1 \end{bmatrix}$,

$$\boldsymbol{R}_{\boldsymbol{A}i}(k) = \begin{bmatrix} \cos\beta_{ik}\cos\gamma_{ik} & \sin\alpha_{ik}\sin\beta_{ik}\cos\gamma_{ik} - \cos\alpha_{ik}\sin\gamma_{ik} & \cos\alpha_{ik}\sin\beta_{ik}\cos\gamma_{ik} + \sin\alpha_{ik}\sin\gamma_{ik} & 0 \\ \cos\beta_{ik}\sin\gamma_{ik} & \cos\alpha_{ik}\cos\gamma_{ik} + \sin\alpha_{ik}\sin\beta_{ik}\sin\gamma_{ik} & \cos\alpha_{ik}\sin\beta_{ik}\sin\gamma_{ik} - \sin\alpha_{ik}\cos\gamma_{ik} & 0 \\ -\sin\beta_{ik} & \sin\alpha_{ik}\cos\beta_{ik} & \cos\alpha_{ik}\cos\beta_{ik} & 0 \\ 0 & 0 & 0 & 1 \end{bmatrix}.$$

Here $[x_{ik}, y_{ik}, z_{ik}]$ represents the coordinates of the rotation center. $\boldsymbol{T}_{\boldsymbol{A}i}(k)$ represents the part translates $-x_{ik}$ along the x-direction, $-y_{ik}$ along the y-direction, and $-z_{ik}$ along the z-direction. $\boldsymbol{R}_{\boldsymbol{A}i}(k)$ represents control point of the ith (i = 1, …, r) part rotates counterclockwise α_{ik} about x axis, β_{ik} about y axis, and γ_{ik} about z axis. Manufacturing part reorientation matrix of station k is shown in Eq. (8):

$$\boldsymbol{A}(k) = \begin{bmatrix} \boldsymbol{A}_1(k) & & & \\ & \boldsymbol{A}_2(k) & & \\ & & \ddots & \\ & & & \boldsymbol{A}_r(k) \end{bmatrix}_{4r \times 4r} \tag{8}$$

If there are r_k parts at station k, it is considered that all the parts involved in the first k–1 stations have been assembled into a sub-structure. As such, the sub-structure is treated as a single object subjecting to reorientation error in subsequent reorientation process at station k, i.e. $\boldsymbol{A}_1(k) = \cdots = \boldsymbol{A}_{r_{k-1}}(k)$. Newly added parts in station k do not undergo reorientation. Hence, $\boldsymbol{A}_{r_{k+1}} = \boldsymbol{A}_{r_{k+2}} = \cdots = \boldsymbol{A}_r = \boldsymbol{O}_{4\times4}$ for these new parts. Note positional deviation is of prime concern during reorientation or re-location process. The deformation (caused by fixture error) is of second order impact in many cases, and it can be modeled using the method presented in Section 3.1 Fixture Error if the deformation impact is material.

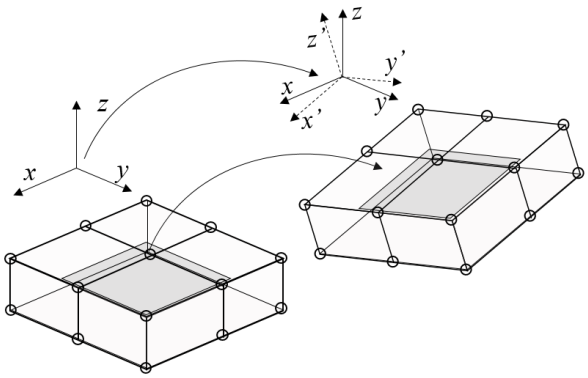

Fig. 2 The reorientation of manufacturing part can be represented through translation and rotation of control points.

4. State-space Model of Compliant Assembly Based on *Parametric Space Envelope (PSE)*

In multi-station assembly, the assembly variation is gradually accumulated through the assembly process, and the assembly at each station can be regarded as a discrete event. Therefore, assembly process can be represented by a state space model [14, 15], as shown in Fig. 3. In contrast, the assembly deviation accumulation process is expressed as the accumulation process of control point displacement under our proposed method. This is shown in Fig. 4 where control point displacement behavior at each station corresponds to a discrete event. Different from existing models (shown in Fig. 3) [14, 15, 33] which track certain feature points on the part state $\boldsymbol{X}(k)$, the deviation transfer in this paper takes the control point state $\boldsymbol{P}(k)$ as the transfer object. The output control point state after assembling at the previous station is the input variable of the current station.

A state space assembly variation transfer model based on *PSE* (parametric space envelope), including state equation and observation equation, is as follows:

$$\begin{aligned} \boldsymbol{P}(k) &= \boldsymbol{A}(k)\boldsymbol{P}(k-1) + \boldsymbol{B}(k)\boldsymbol{U}(k) + \boldsymbol{W}(k) \\ \boldsymbol{Y}(k) &= \boldsymbol{C}(k)\boldsymbol{P}(k) + \boldsymbol{V}(k) \end{aligned} \tag{9}$$

where $\boldsymbol{P}(k)$ represents the control point displacement matrix for every part in the assembly at station k, $\boldsymbol{B}(k)$ is the control matrix, $\mathbf{W}(k)$ the random error at station k, $\boldsymbol{V}(k)$ the observation error, $\boldsymbol{C}(k)$ the observation matrix, and $\mathbf{Y}(k)$ represents the new state of feature points observed for all parts at station k. The state equation transmits locating error, deformation and reorientation error during the assembly process through control points. And the observation equation transforms the control point state into the whole part state at the final station.

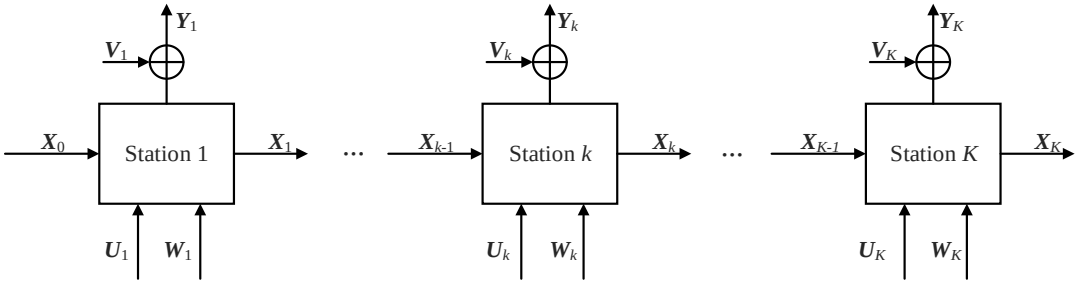

Fig. 3 Current stream-of-variation model of multi-station assembly process.

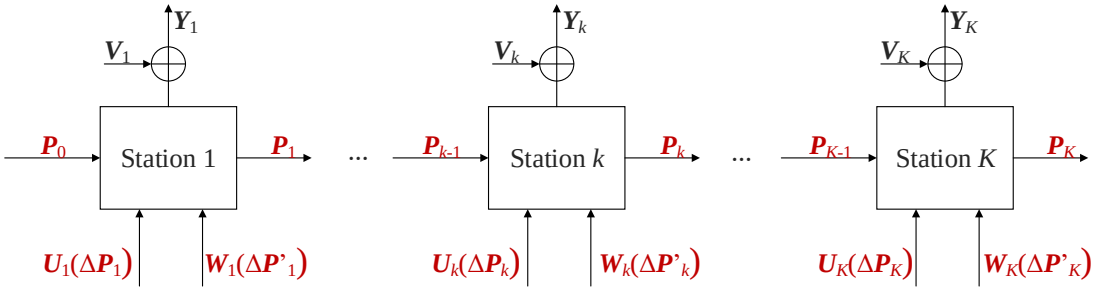

Fig. 4 Multi-station assembly process based on *parametric space envelope* (PSE) technique

4.1 Control Point States. Control point states are matrices that reflect the state of the parts or/and subassemblies, which are objects that are passed along the stations in the multi-station assembly process. The corresponding PSE is constructed according to the shape and complexity of each part, i represents the ith part, and r represents the total number of parts in the assembly process.

$$P_i(k) = \begin{bmatrix} p_{111\mathrm{ix}} & \cdots & p_{\mathrm{lmnix}} & \cdots & p_{\mathrm{Npix}} \\ p_{111\mathrm{iy}} & \cdots & p_{\mathrm{lmniy}} & \cdots & p_{\mathrm{Npiy}} \\ p_{111\mathrm{iz}} & \cdots & p_{\mathrm{lmniz}} & \cdots & p_{\mathrm{Npiz}} \\ 1 & \cdots & 1 & \cdots & 1 \end{bmatrix}_{4\times Npi} \quad i = 1, \cdots, r \tag{10}$$

where p_{lmnix}, p_{lmniy}, and p_{lmniz} represent the state of the (l-m-n)th control point in the x, y, and z directions at station k, respectively. The coordinates of control point in the entire assembly process at station k can be expressed as:

$$\boldsymbol{P}(k) = \begin{bmatrix} \boldsymbol{P}_1(k) & & & \\ & \boldsymbol{P}_2(k) & & \\ & & \ddots & \\ & & & \boldsymbol{P}_r(k) \end{bmatrix}_{4r\times(Np1+\cdots+Npr)} \tag{11}$$

where $\boldsymbol{P}_1(k)$, $\cdots$, $\boldsymbol{P}_r(k)$ represent the coordinates of the control points in the peripheral parameter space of each part. If the number of parts at station k is r_k, the control point state of

the parts not involved in this station is represented with zero matrix, i.e., $\boldsymbol{P}_{r_{k+1}}(k) = \boldsymbol{O}_{4\times Npr_{k+1}}, \cdots, \boldsymbol{P}_r(k) = \boldsymbol{O}_{4\times Npr}$.

4.2 State Equation. During the assembly process, there are two main sources that drive state changes of control points. The first one comes from the activity when the part is transitioned from the $k-1$ station and reoriented at the k station (with the control point following the position of the datum part). The corresponding transformation is represented by the rigid body transformation. The second is from the fact that, when fixture error exists, the locating error changes the control point position and it also causes deformation of the non-rigid part when the part is assembled. According to the above state change sources, the state transfer equation of control point can be established.

During the reorientation process, the position state of control point from station $k-1$ to station k is represented by the coordinate transformation. After reorientation, the coordinates of each control point arrive at new state, and the state coordinates for station k are expressed as:

$$\boldsymbol{P}'(k) = \boldsymbol{A}(k)\boldsymbol{P}(k-1) \tag{12}$$

The movement of each control point state caused by fixture error at station k is as follows:

$$\Delta\boldsymbol{P}(k) = \boldsymbol{B}(k)\boldsymbol{U}(k) \tag{13}$$

where $\boldsymbol{B}(k)$ is the control matrix that expresses the control point displacement $\boldsymbol{U}(k)$ at station k in the coordinate system, as shown in Eq. (14):

$$\boldsymbol{B}(k) = \begin{bmatrix} \boldsymbol{B}_1(k) & & \boldsymbol{O} \\ & \boldsymbol{B}_2(k) & \\ & & \ddots \\ \boldsymbol{O} & & \boldsymbol{B}_r(k) \end{bmatrix}_{4r\times 4r} \tag{14}$$

If the number of existing parts at station k is r_k, then $\boldsymbol{B}_1(k) = \cdots = \boldsymbol{B}_{r_k}(k) = \boldsymbol{I}_{4\times 4}$. The control matrix of parts not involved is represented as zero matrix, i.e. $\boldsymbol{B}_{r_{k+1}} = \boldsymbol{B}_{r_{k+2}} = \cdots = \boldsymbol{B}_r = \boldsymbol{O}_{4\times 4}$.

To account for part variation caused by random errors during assembly, $\boldsymbol{W}(k)$ is introduced and it is assumed to obey a Gaussian distribution with a mean of 0. It is the random incremental movement $\Delta\boldsymbol{P}'(k)$ of each control point. Taking into account all these errors, the new state of the control points at station k is as follows:

$$\begin{aligned} \boldsymbol{P}(k) &= \boldsymbol{P}'(k)+\boldsymbol{B}(k)\boldsymbol{U}(k)+\boldsymbol{W}(k) \\ &= \boldsymbol{A}(k)\boldsymbol{P}(k-1)+\boldsymbol{B}(k)\boldsymbol{U}(k)+\boldsymbol{W}(k) \end{aligned} \tag{15}$$

An example is used to illustrate the locating and reorienting in a typical multi-station assembly shown in Fig. 5. Fig 5(a) shows two parts are assembled in station 1 and the datum part is the left part. Initially the reorientation matrix of the two parts is $\boldsymbol{I}$. Then the locating step causes the right part to deviate from its nominal position. Now the fixture error not only causes a locating error of the part, but also causes deformation of the part. Fig. 5(b) shows the station 2 where the middle part is the datum part. The sub-assembly is reoriented from station 1 to station 2, and the new part (i.e. the right part) at station 2 is located to the nominal position. The fixturing causes deformation of both sub-assembly and the new part. Fig. compares the ideal and real states of the parts after assembly.

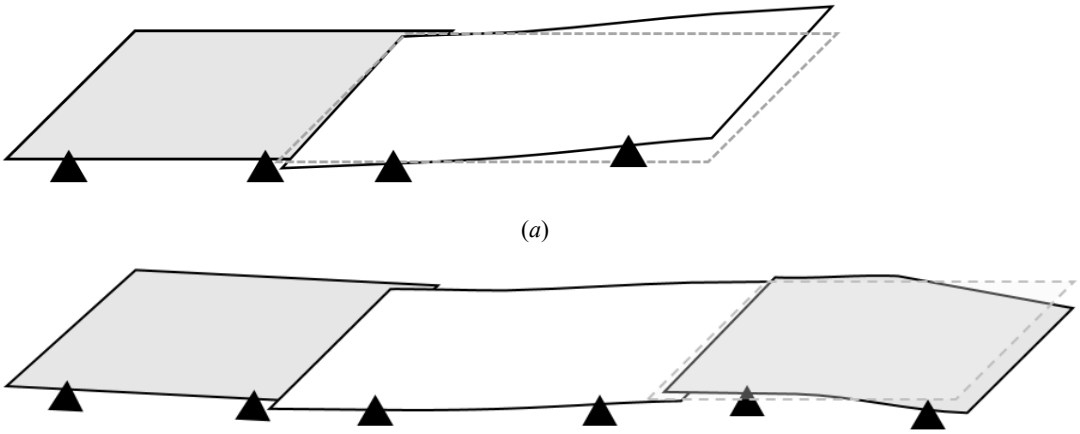

(*a*)

(*b*)

Fig. 5 Two-station assembly: (*a*) two parts are assembled in Station 1, (*b*) extra part is assembled to sub-assembly in Station 2.

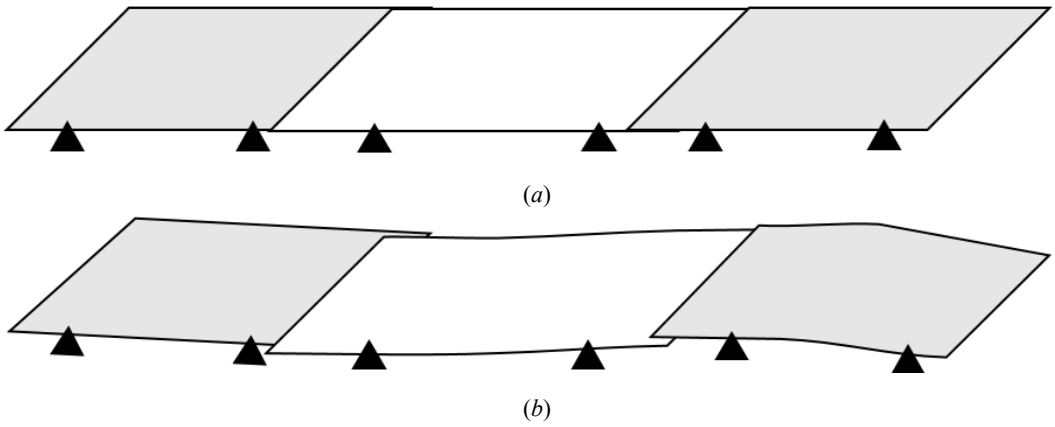

(*a*)

(*b*)

Fig. 6 Assembly results: (*a*) ideal state, (*b*) real state

4.3 Observation Equation. In order to express the observation value of the feature point

$\boldsymbol{Y}(k)$, only the state of the control point in the *x*, *y*, and *z* directions in $\boldsymbol{P}(k)$ is retained in $\boldsymbol{P}(k)$. The control point state $\boldsymbol{P}_i(k)$ of the *i*th part at station *k* is shown in Eq. (16):

$$\boldsymbol{P}_i(k)=\begin{bmatrix} p_{111x} & p_{111y} & p_{111z} \\ \vdots & \vdots & \vdots \\ p_{Npix} & p_{Npiy} & p_{Npiz} \end{bmatrix}_{Npi\times 3} \quad i=1,\cdots,r \tag{16}$$

The control point states of all parts at station *k* are as follows:

$$\boldsymbol{P}(k)=\begin{bmatrix} P_1(k) & & & \\ & P_2(k) & & \\ & & \ddots & \\ & & & P_r(k) \end{bmatrix}_{(Np1+\cdots+Npr)\times 3r} \tag{17}$$

If the number of existing parts at station *k* is r_k, then $P_{r_{k+1}}, P_{r_{k+2}}, \cdots, P_r$ are $\boldsymbol{O}_{Npr_{k+1}\times 3}, \boldsymbol{O}_{Npr_{k+2}\times 3}, \cdots, \boldsymbol{O}_{Npr\times 3}$, respectively.

$\boldsymbol{Y}_i(k)$ represents the state observation value of the *i*th part, including the observed state of all feature points of the part in the coordinate system, that is, the coordinates of the feature points in station *k*. It is a matrix with $h_i\times 3$ dimension, and h_i represents the number of feature points of the *i*th part:

$$\boldsymbol{Y}_i(k)=\begin{bmatrix} y_{1_i x} & y_{1_i y} & y_{1_i z} \\ y_{2_i x} & y_{2_i y} & y_{2_i z} \\ \vdots & \vdots & \vdots \\ y_{h_i x} & y_{h_i y} & y_{h_i z} \end{bmatrix}_{h_i\times 3} \tag{18}$$

where $y_{h_i x}$, $y_{h_i y}$, $y_{h_i z}$, are the components in the *x*, *y* and *z* directions of the *h*th feature point of the *i*th part at station *k*, respectively. The observed state of all parts at station *k* is shown as follows:

$$\boldsymbol{Y}(k)=\begin{bmatrix} \boldsymbol{Y}_1(k) \\ \boldsymbol{Y}_2(k) \\ \vdots \\ \boldsymbol{Y}_r(k) \end{bmatrix}_{(h_1+\cdots h_r)\times 3} \tag{19}$$

$\boldsymbol{Y}(k)$ represents the new state of feature points observed for all parts at station *k*. If the number of existing parts at station *k* is r_k, then $\boldsymbol{Y}_{r_{k+1}}, \boldsymbol{Y}_{r_{k+2}}, \cdots,$ and $\boldsymbol{Y}_r$ are $\boldsymbol{O}_{hr_{k+1}\times 3}, \boldsymbol{O}_{hr_{k+2}\times 3}, \cdots,$ and $\boldsymbol{O}_{hr\times 3}$, respectively.

The observation matrix reflects the influence of control point on the state of the part, and expresses the relationship between the new state of control point and the space state of the part after multi-station assembly. It is composed of Bernstein polynomials:

$$\boldsymbol{C}_i(k)=\begin{bmatrix}\boldsymbol{c}_1\\ \boldsymbol{c}_2\\ \vdots\\ \boldsymbol{c}_{h_i}\end{bmatrix}_{h_i\times Npi} \tag{20}$$

where $\boldsymbol{c}_{ij}=[B_0^{Li}(u)B_0^{Mi}(v)B_0^{Ni}(w),\cdots,B_{Li}^{Li}(u)B_{Mi}^{Mi}(v)B_{Ni}^{Ni}(w)],\ j=1,\ldots,h_i$ .Then the observation matrix at station *k* is shown as follows:

$$\boldsymbol{C}(k)=\begin{bmatrix}\boldsymbol{C}_1(k) & & & \\ & \boldsymbol{C}_2(k) & & \\ & & \ddots & \\ & & & \boldsymbol{C}_r(k)\end{bmatrix}_{(h_1+\cdots+h_r)\times(Np1+\cdots+Npr)} \tag{21}$$

If the number of existing parts at station k is r_k , $\boldsymbol{C}_{r_{k+1}},\boldsymbol{C}_{r_{k+2}},\cdots,$ and $\boldsymbol{C}_r$ are $\boldsymbol{O}_{h_{r_{k+1}}\times Npr_{k+1}},\boldsymbol{O}_{h_{r_{k+2}}\times Npr_{k+2}},\cdots,$ and $\boldsymbol{O}_{h_r\times Npr}$, respectively. Taking into account the observation error $\boldsymbol{V}(k)$, which obeys a Gaussian distribution with a mean value of 0, the state of the part at station *k* can be expressed as follows:

$$\boldsymbol{Y}(k)=\boldsymbol{C}(k)\tilde{\boldsymbol{P}}(k)+\boldsymbol{V}(k) \tag{22}$$

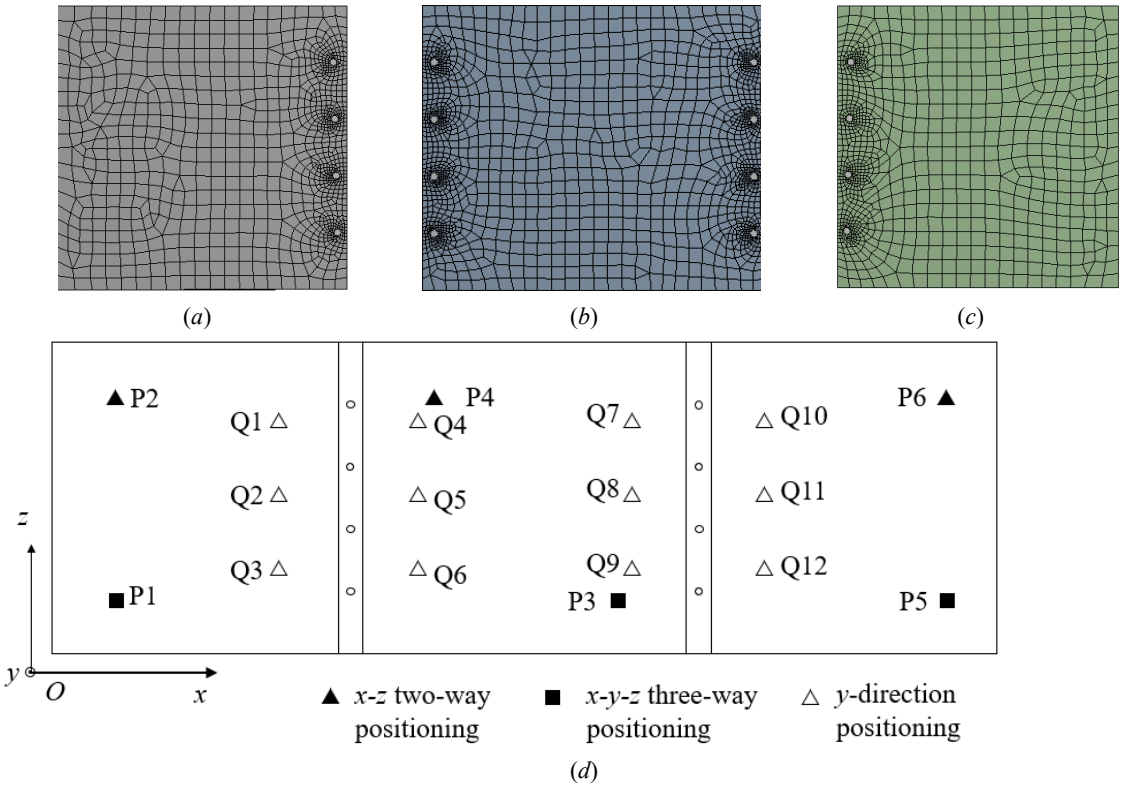

Fig. 7 Three flexible panels to be assembled in two stations: (*a*) the left sheet panel, (*b*) the middle sheet panel, (*c*) the right sheet panel, (*d*) fixturing of the parts during assembly (P stands for positioning while Q represents over-positioning constraint of the panel).

5. Case Study

The proposed methodology is illustrated with an industrial case example of assembling three panels shown in Fig. 7. This process involves two stations and three parts. At Station I,

the left panel (with size of 250 mm × 250 mm) is joined with the middle panel of size 300 mm × 250 mm. Next, in Station II, the subassembly is joined together with the right panel of size 250 mm × 250 mm. The thickness of the panels is 1 mm. The left and the right panels are symmetrical and their deviation during assembly is shown in Fig. 8. The material of every part in the assembly is aluminum alloy with elastic modulus of 71 GPa and Poison's ratio of 0.3. The locating method in this case example is shown in Fig. 7(d).

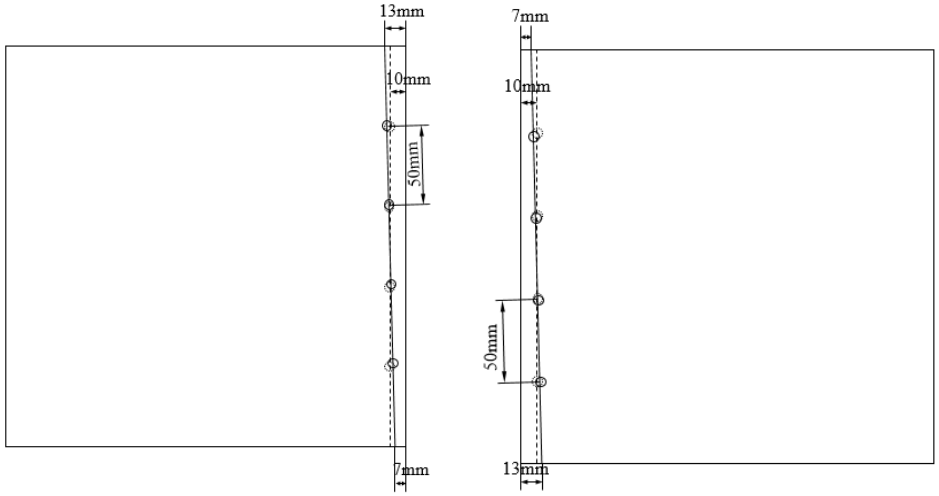

Fig. 8 The left and right panels' deviation during assembly: (*a*) the left panel, (*b*) the right panel

To evaluate the geometric variation for this two stage assembly, the developed methodology is applied. Firstly three PSEs are constructed for the three panels shown in Fig. 9. The starting coordinates and diagonal coordinates of the left, the middle and the right PSEs are [(-390, -135, 1), (-120, 135, 4); (-160, -135, -1), (160, 135, 2); (120, -135, 1), (390, 135, 4)]. And the corresponding control point number in the *x*, *y*, and *z* directions are [(5, 5, 2); (6, 5, 2); (5, 5, 2)] as shown in Fig. 9. Whether the deviation is caused by the reorientation of assembly part or the fixture is shown in Table 1.

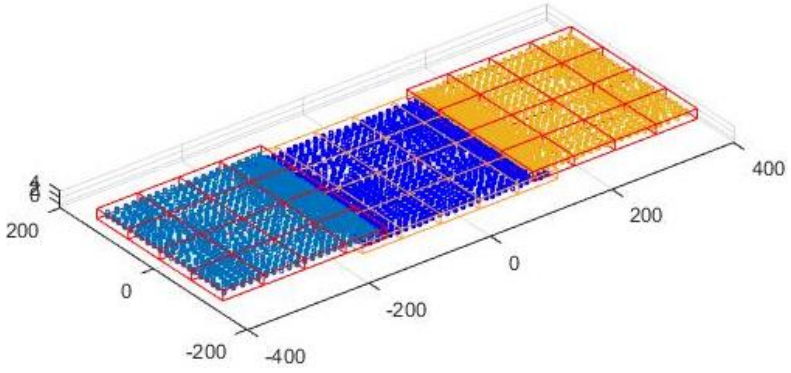

Fig. 9 Constructed parametric space envelopes for the three panels

Table 1 Whether the parts at each station are reoriented, located and deformed

	Part	Reorientation matrix $\boldsymbol{A}$	Position displacement $\boldsymbol{U}1$	Deformation $\boldsymbol{U}2$
Station I	Left panel	identity matrix	√	√
	Middle panel	identity matrix	×	√
Station II	Left panel	identity matrix	×	√
	Middle panel	identity matrix	×	√
	Right panel	identity matrix	√	√

Table 2 Control point input at station I (unit: mm)

	$\boldsymbol{U}1_1(1)$			$\boldsymbol{U}2_1(1)$				$\boldsymbol{U}2_2(1)$		
	x	*y*	*z*	*x*	*y*	*z*		*x*	*y*	*z*
P(1,1,:)*	-3.1671	0	6.0371	0	-0.2208	0	P(1,1,:)	0	0.3441	0
P(2,1,:)	-3.1865	0	4.4176	0	-0.3485	0	P(2,1,:)	0	0.2231	0
P(3,1,:)	-3.2060	0	2.7981	0	-0.4761	0	P(3,1,:)	0	0.1020	0
P(4,1,:)	-3.2254	0	1.1785	0	-0.6039	0	P(4,1,:)	0	-0.0190	0
P(5,1,:)	-3.2448	0	-0.4410	0	-0.7315	0	P(5,1,:)	0	-0.1401	0
P(1,2,:)	-1.5476	0	6.0177	0	-0.1339	0	P(6,1,:)	0	-0.2612	0
P(2,2,:)	-1.5670	0	4.3982	0	-0.2615	0	P(1,2,:)	0	0.4310	0
P(3,2,:)	-1.5864	0	2.7786	0	-0.3893	0	P(2,2,:)	0	0.3099	0
P(4,2,:)	-1.6059	0	1.1591	0	-0.5169	0	P(3,2,:)	0	0.1890	0
P(5,2,:)	-1.6253	0	-0.4604	0	-0.6446	0	P(4,2,:)	0	0.0678	0
P(1,3,:)	0.0720	0	5.9983	0	-0.0470	0	P(5,2,:)	0	-0.0532	0
P(2,3,:)	0.0525	0	4.3787	0	-0.1748	0	P(6,2,:)	0	-0.1743	0
P(3,3,:)	0.0331	0	2.7592	0	-0.3023	0	P(1,3,:)	0	0.5179	0
P(4,3,:)	0.0137	0	1.1397	0	-0.4302	0	P(2,3,:)	0	0.3969	0
P(5,3,:)	-0.0058	0	-0.4799	0	-0.5578	0	P(3,3,:)	0	0.2757	0
P(1,4,:)	1.6915	0	5.9788	0	0.0398	0	P(4,3,:)	0	0.1548	0
P(2,4,:)	1.6721	0	4.3593	0	-0.0877	0	P(5,3,:)	0	0.0336	0
P(3,4,:)	1.6526	0	2.7398	0	-0.2156	0	P(6,3,:)	0	-0.0874	0
P(4,4,:)	1.6332	0	1.1202	0	-0.3432	0	P(1,4,:)	0	0.6048	0
P(5,4,:)	1.6138	0	-0.4993	0	-0.4709	0	P(2,4,:)	0	0.4837	0
P(1,5,:)	3.3110	0	5.9594	0	0.1267	0	P(3,4,:)	0	0.3627	0
P(2,5,:)	3.2916	0	4.3399	0	-0.0010	0	P(4,4,:)	0	0.2415	0
P(3,5,:)	3.2722	0	2.7203	0	-0.1286	0	P(5,4,:)	0	0.1206	0
P(4,5,:)	3.2527	0	1.1008	0	-0.2563	0	P(6,4,:)	0	-0.0006	0
P(5,5,:)	3.2333	0	-0.5187	0	-0.3840	0	P(1,5,:)	0	0.6916	0
/	/	/	/	/	/	/	P(2,5,:)	0	0.5706	0
/	/	/	/	/	/	/	P(3,5,:)	0	0.4495	0
/	/	/	/	/	/	/	P(4,5,:)	0	0.3285	0
/	/	/	/	/	/	/	P(5,5,:)	0	0.2073	0
/	/	/	/	/	/	/	P(6,5,:)	0	0.0863	0

Note: * There are only two layers of control points in Fig. 9. P(1,1,:) refers to upper control point P(1,1,1) and lower control point P(1,1,2). ":" sign in other control points in the table follows similar rule as P(1,1,:) .

There is no reorientation occurs at Station I, so the reorientation matrices $\boldsymbol{A}_i(1)$ for i = 1, 2 are all identity matrices. The initial position of the left panel is the ideal position, but due to the deviation of the rivet hole (Fig. 8(a)), the position deviation of control point $\boldsymbol{U}1_1(1)$ will be generated in order to align the rivet hole during assembly. The compression force and the releasing of the y-direction constraint during assembly deform the panel, so $\boldsymbol{U}2_1(1)$ is not a zero matrix. In Station I assembly, the middle panel is the fixed base part (i.e., no position

Table 3 control point input at station II (unit: mm)

	$\boldsymbol{U}2_1(2)$				$\boldsymbol{U}2_2(2)$				$\boldsymbol{U}1_3(2)$			$\boldsymbol{U}2_3(2)$		
	x	*y*	*z*		*x*	*y*	*z*		*x*	*y*	*z*	*x*	*y*	*z*
P(1,1,:)	0	-1.6753	0	P(1,1,:)	0	-0.7636	0	P(1,1,:)	3.2448	0	-0.441	0	-0.8392	0
P(2,1,:)	0	-1.4077	0	P(2,1,:)	0	-0.5101	0	P(2,1,:)	3.2254	0	1.1785	0	-0.6995	0
P(3,1,:)	0	-1.1403	0	P(3,1,:)	0	-0.256	0	P(3,1,:)	3.206	0	2.7981	0	-0.5593	0
P(4,1,:)	0	-0.8726	0	P(4,1,:)	0	-0.0027	0	P(4,1,:)	3.1865	0	4.4176	0	-0.4198	0
P(5,1,:)	0	-0.6051	0	P(5,1,:)	0	0.2512	0	P(5,1,:)	3.1671	0	6.0371	0	-0.2797	0
P(1,2,:)	0	-1.24	0	P(6,1,:)	0	0.5048	0	P(1,2,:)	1.6253	0	-0.4604	0	-0.317	0
P(2,2,:)	0	-0.9725	0	P(1,2,:)	0	-0.3283	0	P(2,2,:)	1.6059	0	1.1591	0	-0.177	0
P(3,2,:)	0	-0.7044	0	P(2,2,:)	0	-0.0743	0	P(3,2,:)	1.5864	0	2.7786	0	-0.0375	0
P(4,2,:)	0	-0.4375	0	P(3,2,:)	0	0.1787	0	P(4,2,:)	1.567	0	4.3982	0	0.1029	0
P(5,2,:)	0	-0.1696	0	P(4,2,:)	0	0.4333	0	P(5,2,:)	1.5476	0	6.0177	0	0.2426	0
P(1,3,:)	0	-0.8045	0	P(5,2,:)	0	0.6863	0	P(1,3,:)	0.0058	0	-0.4799	0	0.2053	0
P(2,3,:)	0	-0.5368	0	P(6,2,:)	0	0.9403	0	P(2,3,:)	-0.0137	0	1.1397	0	0.345	0
P(3,3,:)	0	-0.2698	0	P(1,3,:)	0	0.1073	0	P(3,3,:)	-0.0331	0	2.7592	0	0.4855	0
P(4,3,:)	0	-0.0015	0	P(2,3,:)	0	0.3605	0	P(4,3,:)	-0.0525	0	4.3787	0	0.6246	0
P(5,3,:)	0	0.2656	0	P(3,3,:)	0	0.6152	0	P(5,3,:)	-0.072	0	5.9983	0	0.7647	0
P(1,4,:)	0	-0.3691	0	P(4,3,:)	0	0.8677	0	P(1,4,:)	-1.6138	0	-0.4993	0	0.7275	0
P(2,4,:)	0	-0.1017	0	P(5,3,:)	0	1.1221	0	P(2,4,:)	-1.6332	0	1.1202	0	0.8676	0
P(3,4,:)	0	0.1663	0	P(6,3,:)	0	1.3756	0	P(3,4,:)	-1.6526	0	2.7398	0	1.007	0
P(4,4,:)	0	0.4333	0	P(1,4,:)	0	0.5425	0	P(4,4,:)	-1.6721	0	4.3593	0	1.1475	0
P(5,4,:)	0	0.7012	0	P(2,4,:)	0	0.7964	0	P(5,4,:)	-1.6915	0	5.9788	0	1.2871	0
P(1,5,:)	0	0.0663	0	P(3,4,:)	0	1.0496	0	P(1,5,:)	-3.2333	0	-0.5187	0	1.2499	0
P(2,5,:)	0	0.3339	0	P(4,4,:)	0	1.3038	0	P(2,5,:)	-3.2527	0	1.1008	0	1.3897	0
P(3,5,:)	0	0.6013	0	P(5,4,:)	0	1.5573	0	P(3,5,:)	-3.2722	0	2.7203	0	1.5297	0
P(4,5,:)	0	0.869	0	P(6,4,:)	0	1.811	0	P(4,5,:)	-3.2916	0	4.3399	0	1.6693	0
P(5,5,:)	0	1.1365	0	P(1,5,:)	0	0.978	0	P(5,5,:)	-3.311	0	5.9594	0	1.8093	0
/	/	/	/	P(2,5,:)	0	1.2317	0	/	/	/	/	/	/	/
/	/	/	/	P(3,5,:)	0	1.4852	0	/	/	/	/	/	/	/
/	/	/	/	P(4,5,:)	0	1.7391	0	/	/	/	/	/	/	/
/	/	/	/	P(5,5,:)	0	1.9927	0	/	/	/	/	/	/	/
/	/	/	/	P(6,5,:)	0	2.2464	0	/	/	/	/	/	/	/

deviation caused by fixture). So $\boldsymbol{U}1_2(1)$ is a zero matrix. After assembly, the *y*-direction constraint (Fig. 7(d)) is released and the panel springback, and the control point will also change accordingly. So $\boldsymbol{U}2_2(1)$ is not a zero matrix.

In Station II, the right panel is joined to the sub-assembly (from Station I) which becomes the assembly base part, reorientation does not occur. The reorientation matrix $\boldsymbol{A}_i(2)$ (i = 1, 2, 3) are all identity matrix. The position of the subassembly does not change from Station I to Station II, so $\boldsymbol{U}1_1(2)$ and $\boldsymbol{U}1_2(2)$ are both zero matrices. The spring back after

assembly at Station II will cause the subassembly to deform, so $\boldsymbol{U}2_1(2)$ and $\boldsymbol{U}2_2(2)$ are not zero matrix. Due to assembly deviation of rivet hole (Fig. 8(b)), control point displacement $\boldsymbol{U}1_3(2)$ will be generated in line with positional deviation of the right panel. Due to the compression force and the release of the y-direction constraint, the right panel experienced deformation. So $\boldsymbol{U}2_3(2)$ is not a zero matrix.

To illustrate and verify the proposed method, FEM is applied using ANSYS software to generate assembly variation shown in Fig. 10 (as proxy to real variation). With assembly variation in Fig. 10, control point displacement can be computed by applying the developed method. $\boldsymbol{U}1_1(1)$ and $\boldsymbol{U}1_3(2)$ are obtained according to the positional relationship of the assembly. $\boldsymbol{U}2_1(1)$, $\boldsymbol{U}2_2(1)$, $\boldsymbol{U}2_1(2)$, $\boldsymbol{U}2_2(2)$ and $\boldsymbol{U}2_3(2)$ are solved by means of generalized inverse matrix with detailed numbers provided in Tables 2 and 3. The assembly variation obtained through the above input variables are shown in Fig. 11. Compared with assembly variation in Fig. 10, the variation results (Fig. 11) produced by the proposed methodology achieves good results from visual inspection. Table 4 provides a quantitative assessment where variation produced from the proposed method only deviates from FEM results by 1.5091×10^{-5} mm on average (for the middle panel).

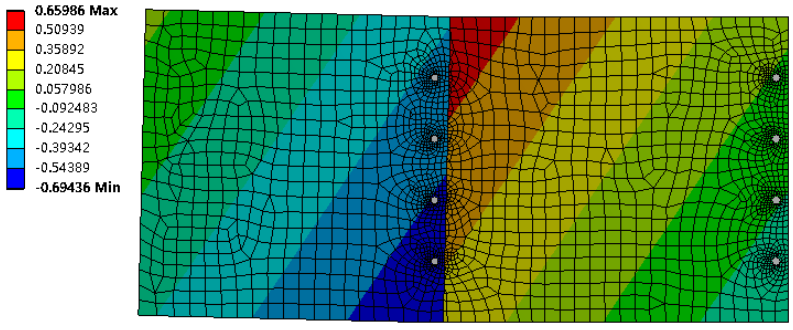

(*a*) Station I

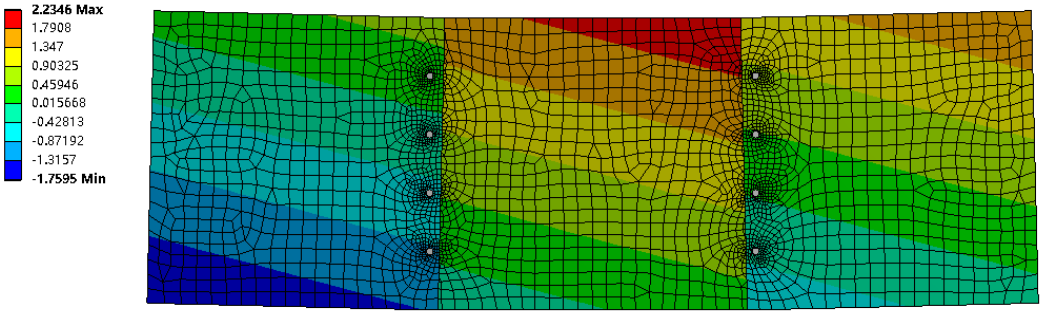

(*b*) Station II

Fig. 10 Assembly variation by the FEM method: (*a*) variation in Station I and (*b*) variation in Station II assembly

Table 4 The difference of produced assembly variation between the proposed method and the FEM method

Unit(mm)	The left panel	The middle panel	The right panel
Max error	7.4651×10^{-5}	6.8628×10^{-5}	7.9698×10^{-5}
Mean error	9.6160×10^{-6}	1.5091×10^{-5}	9.1759×10^{-6}

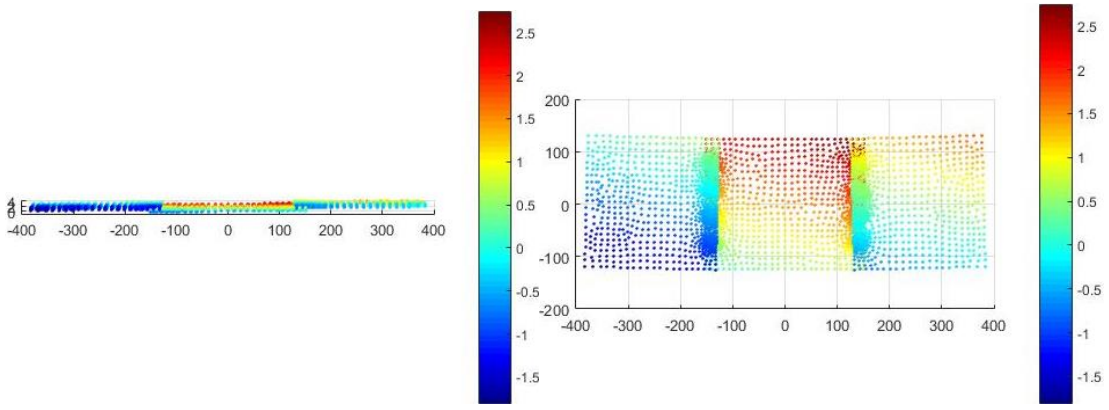

(*a*) (*b*)

Fig. 11 Assembly variation produced by applying the proposed methodology: (a) *xOy* (b) *xOz*

6. Discussion

Using the technique of *parametric space envelope* (PSE), this paper developed a novel geometric variation modeling for multi-station compliant assembly. This research lays the foundation for implementing advanced system identification and control in manufacturing process design, monitoring and diagnosis for compliant assembly. For ease of illustration, the aforementioned parametric space envelope is constructed from Bezier curves. From Eq. (1), modeled variation is impacted by the degree of Bernstein polynomial, the number of control points selected, as well as the positioning of control points. Selecting more control points, i.e., more degrees of freedom, various geometric variation types can be implemented. In practical applications, other parametric curves (i.e., B-splines) can also be chosen to construct the variation tool [41].

In the case study, the control point displacement is derived from assembly variation produced from FEM method. In practical use, real assembly variation can be collected directly from assembly production line [42]. With many real cases, user can produce a distribution of control point displacement at each assembly station. It provides value by analysing the characteristics (i.e. the mean m and the standard deviation σ) of this distribution.

For example, user can conduct variation simulation analysis by simulating control points' movement based on m and σ to generate a large sample of probable variation cases. Analysing this large variation sample, user can identify assembly bottlenecks, adjust assembly procedures, and select proper fixtures to reduce assembly variation in the production run [43]. This aids designers and engineers to make informed decision early on to improve product quality while reduce rework [44, 45]. Further it can aid root cause diagnosis [46, 47, 48].

Existing multi-station assembly variation methods (Fig. 3) track variation propagation through key feature points [14]. To produce a realistic assembly variation for compliant parts, in general it needs to include considerable large amount of feature points resulting in expensive and time-consuming computation [33]. To alleviate this problem, low computation costs simplification methods have been proposed by researchers. One way is to establish a linear model between part deviations and assembly springback deviations by using the method of influence coefficient [17]. In the same vein, Yue et al. [49] proposed a surrogate model to proximate FEM method in an effort to increase dimensional variation prediction accuracy while saving computation costs. In contrast, the proposed method does not involve selecting key feature points and variation modeling is conducted indirectly through a compact set of control points (Fig. 4). To increase modeling accuracy, user only need to add extra several control points around key deformation area (instead of adding hundreds or even thousands of feature points under existing methods). This brings considerable computation efficiency. For the developed method, the bulk calculation involves the cubic B-Spline computation. Many techniques and architectures have been developed in the past decade to improve this computation efficiency [50-53]. Now it is possible to achieve real-time (or near real-time) fast implementation [54].

Today computer-aided systems are widely deployed in industries to enhance product design and manufacturing quality. The modeling methodology developed in this paper is based upon parametric space envelope which is a variation tool constructed from base parametric curves. These parametric curves are routinely used in the computer-aided design (CAD) system [55, 56]. As such, our CAD-driven approach can be integrated into existing CAD, computer-aided manufacturing (CAM) and product lifecycle management (PLM)

systems to facilitate continuous quality improvement to meet industry's rising demands in a new era of digital manufacturing [57, 58].

7. Conclusions and Future Research

This paper presented a new methodology to evaluate assembly variation in a multi-station assembly system where part deformation exists. The methodology is based on *parametric space envelope*, a variation tool constructed to aid geometric variation modeling. For this, geometric variation propagation for flexible parts is modeled indirectly through control points' displacement accumulating through multi-station assembly chain. The proposed method is illustrated and verified through an industrial case example.

Our proposed method holds promising application potential. Equipped with the developed methodology, users can assess assembly variation impact by generating various geometric errors of target assembly by simulating boundary control points' perturbation; User could also link geometric errors pattern of target assembly to assess assembly process capability taking into account various manufacturing requirements. Furthermore, the approach can be applied to analyse and identify the root causes of failed assemblies. We will explore these promising applications in our future research.

In manufacturing and assembly, forces can determine the deformation characteristics of a part. However, real-world forces are not explicitly modeled in the proposed method. The effect of force on deformation is the relationship between the force and the deformation of the workpiece within the elastic range. At present, the most common research on force and deformation is applying finite element analysis, including linear and nonlinear finite element analysis [59]. In our future research, we will study and build the relationship between external assembly load and control points' movement to further enhance the developed methodology.

Acknowledgment

This work was carried out in collaboration with the Digital Lifecycle Management research group from University of Warwick in the UK. This study is also partially supported by the National Natural Science Foundation of China under grant No. 51975119 and No. 51575107 and by UK EPSRC Made Smarter Innovation (MSI) - Research Centre for Smart, Collaborative Industrial Robotics (EP/V062158/1). The support is gratefully acknowledged.

References

[1] Ceglarek, D., Shi, J., 1995, "Dimensional Variation Reduction for Automotive Body Assembly," *Manufacturing Review*, Vol. 8, No. 2, pp. 139 - 154.

[2] Zhong, Z., Mou, S., Hunt, J.H. and Shi, J., 2022, "Finite Element Analysis Model-Based Cautious Automatic Optimal Shape Control for Fuselage Assembly," ASME J. Manuf. Sci. Eng., **144**(8), p.081009.

[3] Wang, H, Ceglarek, D., 2009, "Variation Propagation Modeling and Analysis at Preliminary Design Phase for Multi-station Assembly Systems," *Assembly Automation*, Vol. 29, No. 2, pp. 154-166.

[4] Shi, J. and Zhou, S., 2009. Quality control and improvement for multistage systems: A survey. Iie Transactions, **41**(9), pp.744-753.

[5] Luo, C., Franciosa, P., Ceglarek, D., Ni, Z. and Mo, Z., 2020, "Early stage variation simulation and visualization of compliant part based on parametric space envelope," *IEEE Transactions on Automation Science and Engineering*, **18**(3), pp.1505-1515.

[6] Luo, C., Franciosa, P., Mo, Z. and Ceglarek, D., 2020, "A framework for tolerance modeling based on parametric space envelope," ASME J. Manuf. Sci. Eng., **142**(6), p.061007.

[7] Ceglarek, D., Shi, J., 1996, "Fixture Failure Diagnosis for the Autobody Assembly Using Pattern Recognition," *Trans. of ASME, Journal of Engineering for Industry*, Vol. 118, No. 1, pp. 55-66.

[8] Franciosa, P., Gerbino, S., Ceglarek, D., 2015, "Fixture Capability Optimization for Early-stage Design of Assembly Systems with Compliant Parts using Nested Polynomial Chaos Expansion," Procedia CIRP 41, 87-92,

[9] Luo, C., Wang, X., Su, C. and Ni, Z., 2017, "A fixture design retrieving method based on constrained maximum common subgraph," *IEEE Transactions on Automation Science and Engineering*, **15**(2), pp.692-704.

[10] Luo, C., Zhu, L. and Ding, H., 2011, "Two-sided quadratic model for workpiece fixturing analysis," ASME J. Manuf. Sci. Eng., **133**(3).

[11] Luo, C., Zhu, L. and Ding, H., 2013, "A Unified Distance Function Framework for Workpiece Fixturing Modeling and Analysis," *IEEE Transactions on Automation Science and Engineering*, **10**(4), pp.1166-1172.

[12] Ceglarek, D., Colledani, M., Vancza, J., Kim, D-Y., Marine, C., Kogel-Hollacher, M., Mistry, A., Bolognese, L., 2015, "Rapid Deployment of Remote Laser Welding Processes in Automotive Assembly Systems," *Annals of the CIRP*, Vol. 64/1, pp. 389-394.

[13] Sadeghi Tabar, R., Lorin, S., Cromvik, C., Lindkvist, L., Wärmefjord, K. and Söderberg, R., 2021, "Efficient spot welding sequence simulation in compliant variation simulation," *Journal of Manufacturing Science and Engineering*, *143*(7).

[14] Jin, J. and Shi, J., 1999, "State space modeling of sheet metal assembly for dimensional control," ASME. *J. Manuf. Sci. Eng*., **121**(4): 756–762.

[15] Huang, W., Lin, J., Kong, Z., Ceglarek, D., 2007, "Stream-of-Variation (SOVA) Modeling II: A Generic 3D Variation Model for Rigid Body Assembly in Multistation Assembly Processes," *ASME Trans. on Journal of Manufacturing Science and Engineering,* Vol. 129, No. 4, pp. 832-842.

[16] Wang, K., Li, G., Du, S., Xi, L. and Xia, T., 2021, “State space modelling of variation propagation in multistage machining processes for variable stiffness structure workpieces,” International Journal of Production Research, **59**(13), pp.4033-4052.

[17] Liu, S. C., and Hu, S. J., 1997, “Variation Simulation for Deformable Sheet Metal Assemblies Using Finite Element Methods,” ASME J. Manuf. Sci. Eng., **119**(3), pp. 368–374.

[18] Liu, C., Liu, T., Du, J., Zhang, Y., Lai, X. and Shi, J., 2020, “Hybrid nonlinear variation modeling of compliant metal plate assemblies considering welding shrinkage and angular distortion,” ASME J. Manuf. Sci. Eng., **142**(4).

[19] Ceglarek, D., Shi, J., Wu, S.M., 1994, "A Knowledge-based Diagnosis Approach for the Launch of the Auto-body Assembly Process," *Trans. of ASME, Journal of Engineering for Industry*, Vol. 116, No. 4, pp. 491-499.

[20] Camelio, J., Hu, S.J. and Ceglarek, D., 2003, “Modeling variation propagation of multi-station assembly systems with compliant parts,” J. Mech. Des., **125**(4), pp.673-681.

[21] Ding, Y., Ceglarek, D. and Shi, J., 2000, “Modeling and diagnosis of multistage manufacturing processes: part I state space model,” In *Proceedings of the 2000 Japan/USA symposium on flexible automation* (pp. 23-26). Ann Arbor, MI.

[22] Mantripragada, R. and Whitney, D.E., 1999, “Modeling and controlling variation propagation in mechanical assemblies using state transition models,” *IEEE Transactions on Robotics and Automation*, **15**(1), pp.124-140.

[23] Lawless, J.F., Mackay, R.J. and Robinson, J.A., 1999, “Analysis of variation transmission in manufacturing processes—part I,” Journal of Quality Technology, **31**(2), pp.131-142.

[24] Li, W., Zhang, C., Liu, C. and Liu, X., 2022, “Error propagation model and optimal control method for the quality of remanufacturing assembly,” Journal of Intelligent & Fuzzy Systems, (Preprint), pp.1-15.

[25] Yacob, F. and Semere, D., 2021, “A multilayer shallow learning approach to variation prediction and variation source identification in multistage machining processes,” *Journal of Intelligent Manufacturing*, **32**(4), pp.1173-1187.

[26] Liu, S.C. and Hu, S.J., 1995, “Spot Welding Sequence in Sheet Metal Assembly, Its Analysis and Synthesis,” ASME Manufacturing Science and Engineering, MED, **2**(2), pp.1145-1156.

[27] Shahi, V.J., Masoumi, A., Franciosa, P. and Ceglarek, D., 2020, “A quality-driven assembly sequence planning and line configuration selection for non-ideal compliant structures assemblies,” *The International Journal of Advanced Manufacturing Technology*, *106*, pp.15-30.

[28] Chang, M. and Gossard, D.C., 1997, “Modeling the assembly of compliant, non-ideal parts,” *Computer-aided design*, **29**(10), pp.701-708.

[29] Liu, S.C., Hu, S.J. and Woo, T.C., 1996, “Tolerance analysis for sheet metal assemblies,” ASME. *J. Mech. Des*., **118**(1): 62–67.

[30] Li, Z., Kokkolaras, M., Papalambros, P. and Hu, S.J., 2008, "Product and process tolerance allocation in multistation compliant assembly using analytical target cascading," J. Mech. Des., **130**(9): 091701.

[31] Huang, W. and Ceglarek, D., 2002, "Mode-based decomposition of part form error by discrete-cosine-transform with implementation to assembly and stamping system with compliant parts," CIRP Annals, **51**(1), pp.21-26.

[32] Huang W., Liu, J., Chalivendra, V., Ceglarek, D., Kong, Z., Zhou, Y., 2014, "Statistical Modal Analysis (SMA) for Variation Characterization and Application in Manufacturing Quality Control," *IIE Transactions,* Vol. 46, Issue 5, pages 497-511

[33] Camelio, J.A., Hu, S.J. and Marin, S.P., 2004, "Compliant assembly variation analysis using component geometric covariance," J. Manuf. Sci. Eng., **126**(2), pp.355-360.

[34] Shi, J., 2006, *Stream of variation modeling and analysis for multistage manufacturing processes*. CRC press.

[35] Zhang, T. and Shi, J., 2016, "Stream of variation modeling and analysis for compliant composite part assembly—Part II: Multistation processes," J. Manuf. Sci. Eng., **138**(12): 121004.

[36] Jandaghi Shahi, V. and Masoumi, A., 2020, "Integration of in-plane and out-of-plane dimensional variation in multi-station assembly process for automotive body assembly," Proceedings of the Institution of Mechanical Engineers, Part D: Journal of Automobile Engineering, **234**(6), pp.1690-1702.

[37] Franciosa P., Ceglarek D. VRM 3.0 (Variation response method) (2018) https://warwick.ac.uk/fac/sci/wmg/research/manufacturing/downloads/

[38] Franciosa, P., Palit, A., Gerbino, A., Ceglarek, D., 2019, "A Novel Hybrid Shell Element Formulation (QUAD+ and TRIA+): A Benchmarking and Comparative Study," *Finite Elements in Analysis and Design*, Vol. 166, Article No. UNSP 103319, November 2019, DOI: https://doi.org/10.1016/j.finel.2019.103319.

[39] Luo, C., Franciosa, P., Ceglarek, D., Ni, Z. and Jia, F., 2018, "A novel geometric tolerance modeling inspired by parametric space envelope," IEEE Transactions on Automation Science and Engineering, **15**(3), pp.1386-1398.

[40] Shiu, B.W., Ceglarek, D. and Shi, J., 1996, "Multi-stations sheet metal assembly modeling and diagnostics," *TRANSACTIONS-NORTH AMERICAN MANUFACTURING RESEARCH INSTITUTION OF SME*, pp.199-204.

[41] Song, C., Zhou, Y. and Luo, C., 2019, "Geometric tolerance modeling method based on B-spline parameter space envelope," In *2019 IEEE International Conference on Mechatronics and Automation (ICMA)* (pp. 2058-2063). IEEE.

[42] Babu, M.K., Franciosa, F., Ceglarek, D., 2019, "Spatio-Temporal Adaptive Sampling for Effective Coverage Measurement Planning during Quality Inspection of Free-Form Surfaces using Robotic 3D Optical Scanner," Journal of Manufacturing Systems. Vol. 53, pp. 93-108, October 2019,

https://doi.org/10.1016/j.jmsy.2019.08.003.

[43] Lorin, S., Lindau, B., Lindkvist, L. and Söderberg, R., 2019, "Efficient compliant variation simulation of spot-welded assemblies," Journal of Computing and Information Science in Engineering, **19**(1).

[44] Yu, H., Zhao, C. and Lai, X., 2018, "Compliant assembly variation analysis of scalloped segment plates with a new irregular quadrilateral plate element via ANCF," Journal of Manufacturing Science and Engineering, **140**(9).

[45] Djurdjanovic, D., Mears, L., Niaki, F.A., Haq, A.U. and Li, L., 2018, "State of the art review on process, system, and operations control in modern manufacturing," Journal of Manufacturing Science and Engineering, **140**(6).

[46] Kong, Z., Ceglarek, D. and Huang, W., 2008, "Multiple fault diagnosis method in multistation assembly processes using orthogonal diagonalization analysis," J. Manuf. Sci. Eng., **130**(1).

[47] Ding, Y., Shi, J. and Ceglarek, D., 2002, "Diagnosability analysis of multi-station manufacturing processes," J. Dyn. Sys., Meas., Control, **124**(1), pp.1-13.

[48] Sinha, S., Franciosa, P., Ceglarek, D., 2021, "Object Shape Error Response using Bayesian 3D Convolutional Neural Networks for Root Cause Analysis of Manufacturing Systems," IEEE Transactions on Industrial Informatics, Vol. 17, No. 10, pp. 6676-6686, DOI: 10.1109/TII.2020.3043226, October.

[49] Yue, X., Wen, Y., Hunt, J.H. and Shi, J., 2018, "Surrogate model-based control considering uncertainties for composite fuselage assembly," J. Manuf. Sci. Eng., **140**(4): 041017.

[50] Modat, M., Ridgway, G.R., Taylor, Z.A., Lehmann, M., Barnes, J., Hawkes, D.J., Fox, N.C. and Ourselin, S., 2010, "Fast free-form deformation using graphics processing units," Computer methods and programs in biomedicine, **98**(3), pp.278-284.

[51] Cui, Y. and Feng, J., 2013, "Real-time B-spline Free-Form Deformation via GPU acceleration," Computers & graphics, **37**(1-2), pp.1-11.

[52] Wang, Y., Jacobson, A., Barbič, J., and Kavan, L., 2015, "Linear subspace design for real-time shape deformation," ACM Transactions on Graphics (TOG), **34**(4), 1-11.

[53] Palomar, R., Gómez-Luna, J., Cheikh, F.A., Olivares-Bueno, J. and Elle, O.J., 2018, "High-performance computation of bézier surfaces on parallel and heterogeneous platforms," International Journal of Parallel Programming, **46**(6), pp.1035-1062.

[54] Akenine-Moller, T., Haines, E. and Hoffman, N., 2019. *Real-time rendering*. AK Peters/crc Press.

[55] Farin, G., 2014, *Curves and surfaces for computer-aided geometric design: a practical guide*. Elsevier.

[56] Bi, Z. and Wang, X., 2020. *Computer aided design and manufacturing*. John Wiley & Sons.

[57] Ramanujan, D., Bernstein, W., Diaz-Elsayed, N. and Haapala, K.R., 2022, "The Role of Industry 4.0 Technologies in Manufacturing Sustainability Assessment," J. Manuf. Sci. Eng., pp.1-64.

[58] Ghobakhloo M., 2020, "Industry 4.0, digitization, and opportunities for sustainability," *Journal of cleaner production*; 252:119869.

[59] Hughes, T.J., 2012. *The finite element method: linear static and dynamic finite element analysis*. Courier Corporation.